

Contrasting terrace systems of the lower Moulouya river as indicator of crustal deformation in NE Morocco



Gilles Rixhon ^{a,*}, Melanie Bartz ^a, Meriam El Ouahabi ^b, Nina Szemkus ^a, Helmut Brückner ^a

^a Institute for Geography, University of Cologne, Zùlpicher Straße 45, 50674 Cologne, Germany

^b Department of Geology, University of Liège, Allée du six Août 14, 4000 Liège, Belgium

ARTICLE INFO

Article history:

Received 23 December 2015

Received in revised form

4 November 2016

Accepted 7 November 2016

Available online 9 November 2016

Keywords:

Fluvial terraces

River sediments

Late Cenozoic

Thrust zone

Moulouya river

North-eastern Morocco

ABSTRACT

The Moulouya river has the largest catchment in Morocco and drains an area characterized by active crustal deformation during the Late Cenozoic due to the N–S convergence between the African and Eurasian plates. As yet, its Pleistocene terrace sequence remains poorly documented. Our study focuses on the lowermost reach of the river in north-eastern Morocco, which drains the Zebra-Triffa sedimentary basin directly upstream of the estuary. New field observations, measurements and sedimentological data reveal contrasting fluvial environments on each side of a newly identified, W–E striking thrust zone disrupting the sedimentary basin. On the one hand, long-lasting fluvial aggradation, materialized by 37 m-thick stacked terraces, has occurred in the footwall of the thrust. On the other hand, the hanging wall is characterized by a well-preserved terrace staircase, with three Pleistocene terrace levels. Whilst the identification of this thrust zone questions some previous interpretations about the local (hydro-) geology, it is consistent with the statement that most of the Plio-Quaternary deformation in the eastern Rif mountains has concentrated in this region of Morocco. Our new data and interpretations also agree with morphometric indicators showing that the whole Moulouya catchment is at disequilibrium state (i.e. several knickzones in its longitudinal profile), showing several knickzones in its longitudinal profile, is at disequilibrium state. We also suggest that the knickzone in the Beni Snassen gorge, located directly upstream of the Zebra-Triffa sedimentary basin, could (partly) result from a transient fluvial reaction to Late Cenozoic thrusting activity and correlated uplift in the hanging wall.

© 2016 Elsevier Ltd. All rights reserved.

1. Introduction

Located in the convergence zone between the African and Eurasian plates, the northern part of Morocco represents an area of active crustal deformation during the Late Cenozoic (e.g. Meghraoui et al., 1996). The 1994–2004 Al Hoceima earthquake sequence is evidence of the active seismicity of this region (e.g. Akoglu et al., 2006). Whilst seismicity was investigated by diverse methods, for instance radar interferometry (Akoglu et al., 2006), the reconstruction of Late Cenozoic and modern rates of crustal deformation is mainly based on GPS measurements (Fadil et al., 2006; Vernant et al., 2010), morphotectonics (i.e. displacement of geomorphological markers: Poujol et al., 2014; Pastor et al., 2015), and morphometric indicators (Barcos et al., 2014).

Morphometric indicators show that most of the fluvial systems draining the north-eastern part of Morocco are in disequilibrium (Barcos et al., 2014). This is especially true for the ~74,000 km² large Moulouya catchment, the second largest fluvial system of North Africa debouching into the Mediterranean Sea after the Nile. As a result of ongoing N–S compressive shortening in north-eastern Morocco, Barcos et al. (2014) also postulate that the main W–E striking deformational front between the Rif belt and the Atlas mountains stretches across the lowermost 65 km-long valley reach of the Moulouya river, the so-called Zebra-Triffa sedimentary basin. Even though river terrace sequences generally represent useful indicators to detect crustal deformation (e.g. Demir et al., 2012), the fluvial sedimentary record of the Moulouya remains poorly documented. Excepted a few studies about Late Cenozoic deposits in its middle reach (Raynal, 1961; Lefèvre, 1984, 1989), a reliable reconstruction of the Quaternary terraces along the entire river course is still lacking. As for the lowermost valley reach, where most of the recent

* Corresponding author.

E-mail address: grixhon@uni-koeln.de (G. Rixhon).

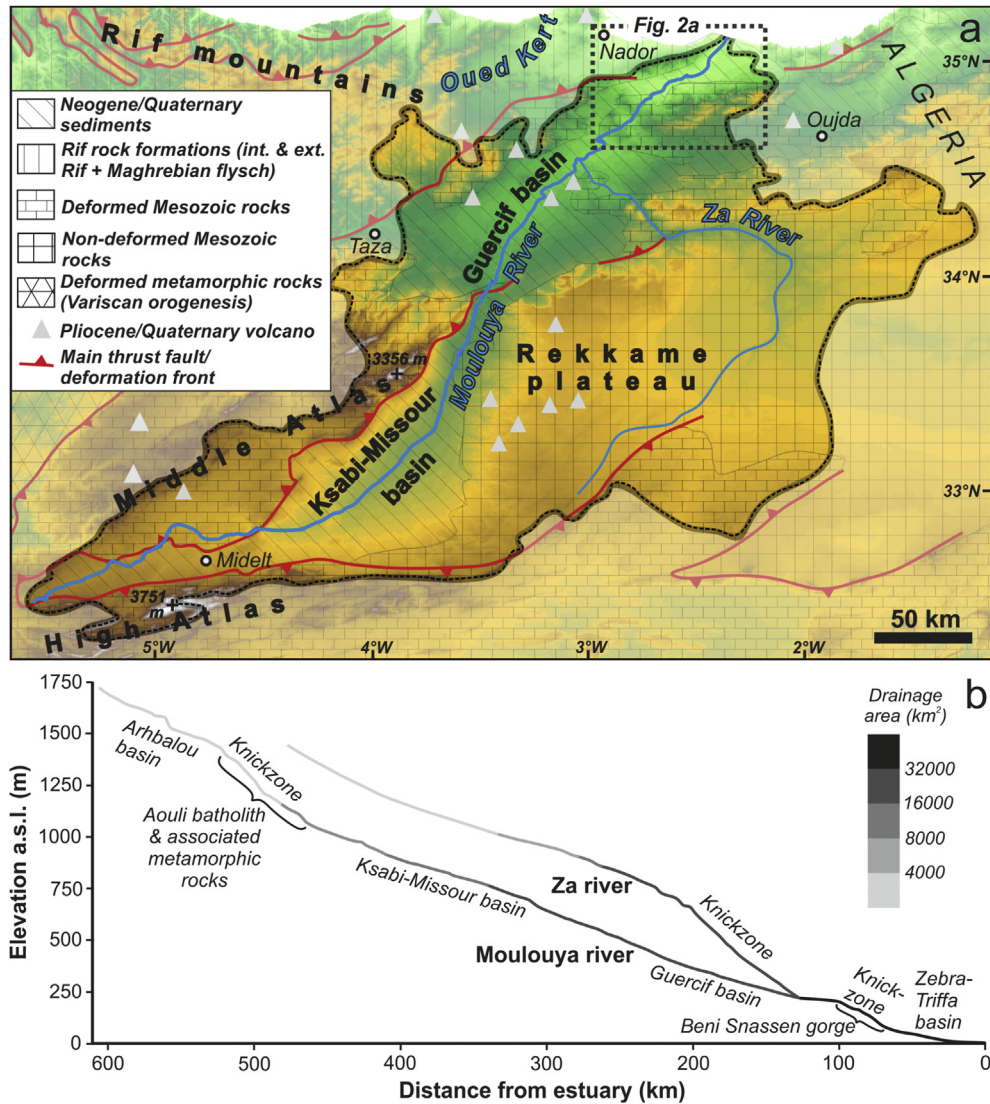


Fig. 1. (A) Relief map of the Moulouya catchment (delimited by black dashed line), with the main regional geological structures of northern Morocco (according to Barcos et al., 2014). The dashed rectangle refers to the zoom in of the lower Moulouya (Fig. 2A). (B) Longitudinal profiles of the Moulouya river and its main tributary, the Za river, with location of the main sedimentary basins and knickzones. Modified after Pastor et al. (2015).

geomorphological and stratigraphical research took place, all studies exclusively focused on the Holocene sedimentary record to infer climatic and human-induced changes (Ibouhouten et al., 2010; Zielhofer et al., 2008, 2010), eustatic variations (Pissart and Boumeaza, 2010) or tectonic deformation (Zarki et al., 2004). However, the distribution of these (almost) continuous Holocene overbank fine-grained sediments along this reach was either not mapped (Ibouhouten et al., 2010; Zielhofer et al., 2008, 2010) or at a very poor resolution (Pissart and Boumeaza, 2010). Even more problematic is the fact that Pleistocene terrace sediments in the previous studies were either completely disregarded (Ibouhouten et al., 2010; Zielhofer et al., 2008, 2010) or erroneously interpreted as Pliocene marine conglomerates (Pissart and Boumeaza, 2010).

Therefore, this study first aims at (i) providing a comprehensive image of the river terraces' distribution, including changes in the valley morphology, and (ii) establishing a relative stratigraphy of Late Cenozoic landforms in the lowermost Moulouya reach. To achieve these goals, we conducted a field survey based on profile description and geomorphological mapping using a differential global positioning system (DGPS) and a laser distance meter. In two selected profiles, clast lithological analysis and measurements of

carbonate contents were carried out to investigate the sedimentary environment and the post-depositional evolution of the river deposits. Field survey was supplemented by the analysis of satellite images. Finally, the reconstruction of the Quaternary fluvial environments in the lower Moulouya reach was used to better understand the position of the deformational front in this sedimentary basin and the resulting fault pattern.

2. Study area

2.1. Geodynamic background of north-eastern Morocco

In the northern part of Morocco, there is a general consensus to consider N–S compressive shortening as the main geodynamic process from the Miocene to the Quaternary. Ait Brahim et al. (2002) showed that Messinian sedimentary sequences are affected by N–S to N140° E compression in the eastern Rif belt and that Middle Pleistocene terrace sequences in the region of Oujda and of the Oued Kert, located eastward and westward of the Moulouya, respectively, were deformed (Fig. 1A). Based on kinematic analyses of Pliocene and Quaternary fault systems in the Rif

mountains, a N–S to NW–SE main compressional stress direction, associated with shortening rates of 1–2.3 mm/yr, was suggested (Meghraoui et al., 1996). Recently, trend-topography surface analysis highlighted an E–W trending lithospheric dome in the eastern Rif and in the Beni Snassen massif (Barcos et al., 2014). Morphometric indicators also revealed active deformations accommodating a N–S shortening at the northern margin of the Beni Snassen massif (Barcos et al., 2014). At last, recent geodetic observations evidenced a southward motion of the Rif mountains (~3 mm/a) relative to the interior of the African plate (Fadil et al., 2006; Vernant et al., 2010).

2.2. The Moulouya catchment

2.2.1. General hydro-geomorphological setting

Originating in the southern part of the Middle Atlas, the >600 km-long, SW–NE oriented Moulouya river represents the second largest fluvial system of North Africa draining into the Mediterranean Sea (Fig. 1A). With a catchment area of ~74,000 km² (Pastor et al., 2015), its river network drains the northernmost part of the High Atlas to the south, the High plateaus to the east, the eastern half of the Middle Atlas to the west and the south-eastern margin of the Rif mountains to the north (Fig. 1A). The main trunk flows across several intramontane basins filled with Neogene sediments. From source to mouth, they are the Arhbalou, Ksabi-Missour, Guercif and Zebra-Triffa-Ouled Mansour basins, the last one being located directly upstream of the river estuary (Fig. 1A and B). Morphometric indicators along with deformations of the drainage network and the presence of large knickzones in the Moulouya catchment point to a disequilibrium state (Fig. 1B; Barcos et al., 2014; Pastor et al., 2015). The catchment shows an S-shaped hypsometric curve and has a hypsometric value of 0.313, while the normalized stream-length gradient index (SLk) points to high anomalies along the entire river course (Barcos et al., 2014).

The Moulouya catchment is characterized by a semi-arid to arid Mediterranean climate. Average precipitations range from 150 to 600 mm between the basin lowlands and the Atlas Mountains (Kaemmerer and Revel, 1991). Highest fluctuations of the water discharge occur from October to January; they are generally related to heavy rainfall events, usually very concentrated in time (Snoussi et al., 2002). This results in very high peak discharges: e.g. ~5200 m³/s for the 1963 flood event (i.e. >200 times greater than the mean annual discharge; Snoussi et al., 2002; Zielhofer et al., 2008).

2.2.2. The middle reaches (Ksabi-Missour basin)

In the High and Middle Atlas regions, two main processes resulted in rock uplift: thrusting due to tectonic shortening, active since the Paleogene, and long-wavelength surface uplift due to mantle-driven buoyancy since the Late Cenozoic (Babault et al., 2008). In the Ksabi basin (Fig. 1A), the existence of a Quaternary terrace staircase, encompassing up to eight distinct levels, and stacked terraces were recognized (Raynal, 1961; Lefèvre, 1989; Kaemmerer and Revel, 1991). The landscape is characterized by a tight inter-fingering between alluvial deposits of the Moulouya and footslope sedimentation landforms (alluvial cones, glacia), the latter usually capping the river sediments (Lefèvre, 1989). Further to the north in the Missouri basin (Fig. 1A), recent ¹⁰Be dating of fluvial landforms, i.e. terrace fans from a tributary of the Moulouya draining the eastern flank of the Middle Atlas, allowed inferring incision rates of ~0.3 mm/a, implying that mantle-driven uplift amounted to ~0.1–0.2 mm/a during the Middle Pleistocene (Pastor et al., 2015).

2.2.3. The lowermost reach: the Zebra-Triffa-Ouled Mansour sedimentary basin

Downstream of the 30 km-long gorge cut into the Beni Snassen

massif (see below) until the estuary, the ~65 km-long reach of the Moulouya successively drains the so-called Zebra plain, Triffa plain and Ouled Mansour plateau (Fig. 2A). For clarity, the geologic basin formed by these three geographic areas will be named lowermost sedimentary basin in the following text. It is a large WSW–ENE striking synclinal depression mostly filled with Neogene marine deposits (Ruellan, 1971; Boughriba et al., 2006). As a component of the larger-scale Melilla basin, it emerged around 3.6 Ma (Rouchy et al., 2003). This synclinal structure is bordered by two complex, generally WSW–ENE striking anticlinal ridges: the Beni Snassen and the Kbdana mountains to the south and the north, respectively (Fig. 2A). Both massifs are primarily formed by diverse Mesozoic carbonate rocks, including limestone, dolomite, dolomitic limestone, calcareous marl and sandstone, and marl (Ruellan, 1971). They are secondarily composed of sandstone and slate formations of the Palaeozoic flysch series (Ruellan, 1971; Khattach et al., 2004).

Located to the north of the Triffa plain (Fig. 2A), the up to 10 km-wide and up to 130 m-high Ouled Mansour plateau is mostly formed of Mio-Pliocene marls and partly solidified sands (Ruellan, 1971). Despite many recent geological or geophysical studies, mostly dealing with the hydrogeology of the lowermost part of the Moulouya catchment (e.g. Khattach et al., 2004; Boughriba et al., 2006; Chennouf et al., 2007a,b; Fetouani et al., 2008; Sardinha et al., 2012), the geological structure of the Ouled Mansour plateau remains confusing. This is especially true for the >20 km-long, continuous lineament at its southern edge (Fig. 2A). Whilst the latter was traditionally mapped as a flexural feature (e.g. Ruellan, 1971; Boughriba et al., 2006; Fetouani et al., 2008), Khattach et al. (2004) and Chennouf et al. (2007a) interpreted the Ouled Mansour plateau as a Miocene horst, thereby implying the presence of normal faults at its borders. In this respect, several WSW–ENE striking fault lines stretching across the Triffa-Ouled Mansour area are represented on the neotectonic map of Morocco (Faure-Muret and Morel, 1994). However, their exact position remains somewhat imprecise given the 1:1,000,000 scale of the map, and the nature of fault motion remains unknown. A SW–NE striking deformational front between the Rif belt and the Atlas mountains through the lowermost sedimentary basin of the Moulouya was assumed on the structural map of Morocco (Saadi, 1982). This main deformational front is also postulated by Barcos et al. (2014) but has a W–E orientation and a different extension. Note finally that these last authors reported active faulting, both normal and reverse, affecting Quaternary river deposits at the northern rim of the Beni Snassen massif (i.e. the lowermost Moulouya catchment, Fig. 2A) but without any precision about the location and the extension of these faults.

In the lowermost reach of the Moulouya, the up to 15 m-thick recent flood deposits are formed of unconsolidated clayey/silty/sandy laminae spanning the whole Holocene period (Zielhofer et al., 2008, 2010; Ibouhouten et al., 2010; Pissart and Boumeaza, 2010). For clarity, these sediments, which are not in the focus of this study, will be referred to as Holocene overbank fines in the following. Up to three distinct erosional terraces were carved into these overbank fines during a stepwise Holocene river incision according to Pissart and Boumeaza (2010). The detailed chronostratigraphic study of this sedimentary record, along with palaeoecological proxies, allowed inferring its strong coupling with Holocene rapid climate changes (Zielhofer et al., 2008, 2010; Ibouhouten et al., 2010), although this was formerly contested by Zarki et al. (2004). At last, abundant archaeological material along with fire places found in these sediments reveal temporary human settlements along the lower Moulouya (Fig. 2B; Ibouhouten et al., 2010; Linstädter et al., 2012), with a peak of human presence during the Epipalaeolithic (~7.8–10.1 ka cal BP) and the Neolithic (~5.5–7.4 ka cal BP).

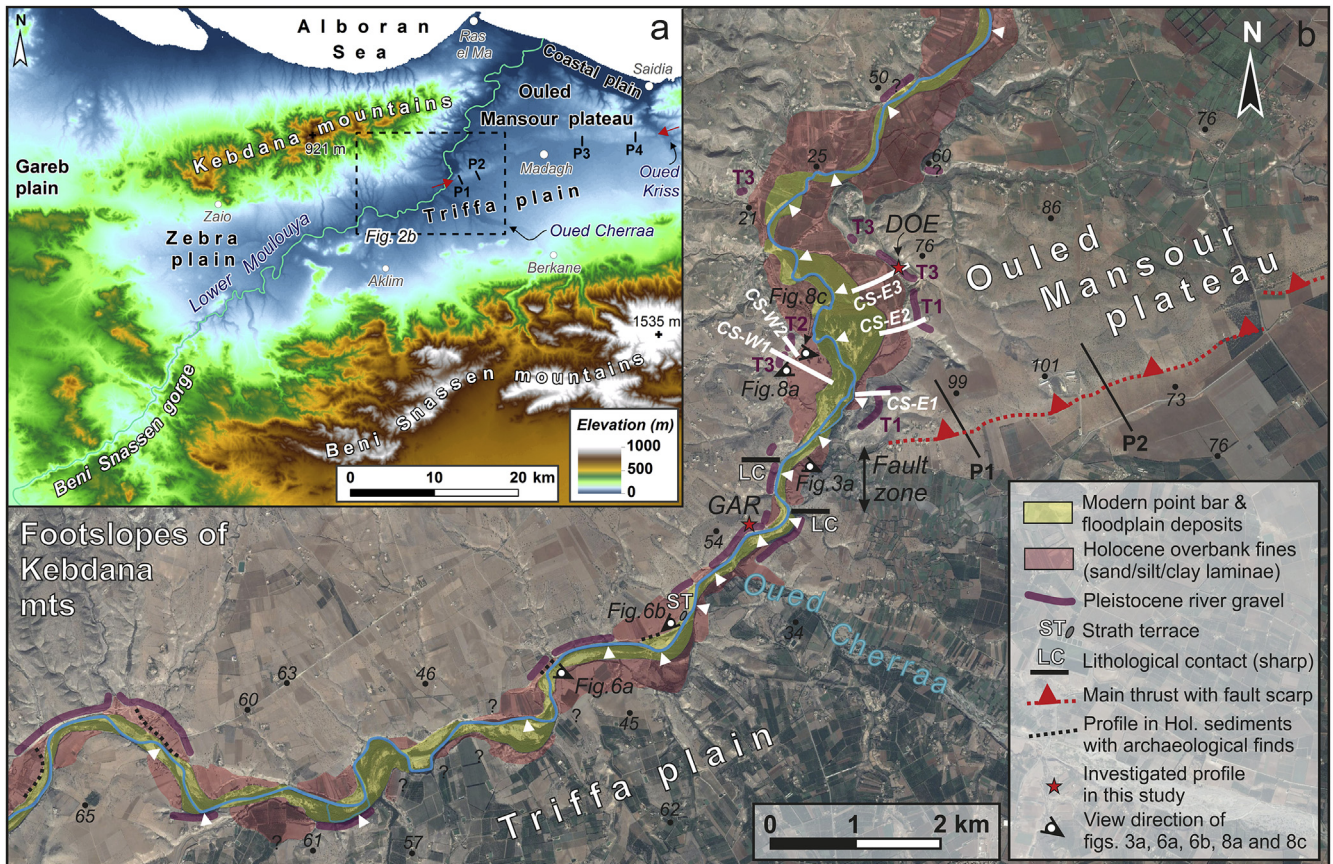


Fig. 2. (A) SRTM-based DEM of the lower Moulouya catchment, showing the Beni Snassen gorge and the ~65 km-long river reach draining the lowermost sedimentary basin (Zebra plain-Triffa plain-Ouled Mansour plateau). The red arrows refer to the continuous fault scarp at the southern edge of the Ouled Mansour plateau and P1 to P4 locate the cross sections represented in Fig. 4. The dashed rectangle refers to our study area. (B) The 20 km-long studied valley reach of the lower Moulouya with main morphological and geological features as well as profiles described in the text (satellite image: Google Earth, CNES/Astrium, 02.08.2014). White triangles refer to the locations where valley and floodplain width measurements were performed (see Fig. 5A). DGPS cross sections (CS) are represented by bold white lines and were performed both on the eastern (E1–3) and western (W1–2) valley sides (see Fig. 9). Small black circles with numbers are absolute elevations according to topographic points mentioned on Moroccan 1:50,000 topographic maps. T1, T2 and T3 refer to the Pleistocene terrace levels characteristic of the hanging wall reach (see text and Figs. 8, 9, 11). Uncertain extension of fluvial units is symbolised by question marks. Details about the profiles in Holocene sediments with archaeological finds can be found in Zielhofer et al. (2008, 2010) and Linstädter et al. (2012). (For interpretation of the references to colour in this figure legend, the reader is referred to the web version of this article.)

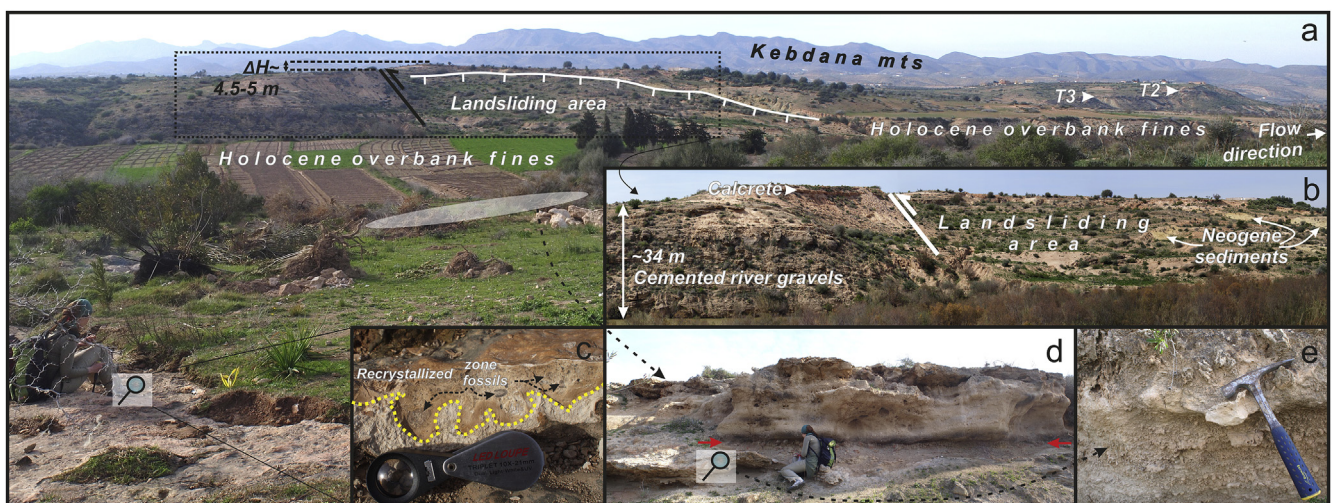


Fig. 3. (A) Panorama view of the western valley side in the fault zone, characterized by an up to 330 m-long landsliding area (scarp delimited by white line), stretching to the current channel. Note also the sharp 4.5–5 m-high vertical offset (ΔH) at the western tip of this area, where the presumed thrust zone (black line with arrow) occurs. T2 and T3 refer to two distinct terrace levels observed in the terrace staircase downstream (see 4.3.1.). (B) Detailed view of the western valley side, exhibiting a lithological transition, along flow direction, between 34 m-thick river gravels sealed by a calcrete and Neogene marine deposits, locally observable in the landsliding area. (C) Neogene marine deposits: contact between unaltered carbonates (light greyish zone) and recrystallized carbonates with fossils at the ground surface of the eastern valley side. (D) Fossil-rich outcrop in the upper part of the eastern valley wall. Note the blackish zone (red arrows), attesting for recrystallization of the shelly carbonate layers. (E) Close-up of the marine fossils (shell fragments mostly). (All photos: G. Rixhon). (For interpretation of the references to colour in this figure legend, the reader is referred to the web version of this article.)

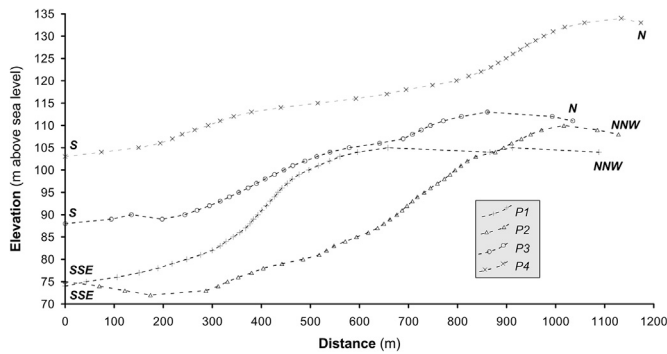


Fig. 4. Topographic cross sections at the southern edge of the Ouled Mansour plateau (location on Fig. 2A).

3. Material and methods

This study tests the hypothesis of Barcos et al. (2014) of a main deformational front related to ongoing N–S compression disrupting the lowermost sedimentary basin of the Moulouya: the presence of a thrust zone at the transition between the Triffa plain to the south and the Ouled Mansour plateau to the north is thus postulated. For clarity in the following text, the river reach draining the Triffa plain is assimilated to the footwall and the one draining the Ouled Mansour plateau to the hanging wall. A detailed discussion about the thrust zone is provided in section 5.3.

Field survey included geomorphological mapping and the description and sampling of two profiles along the ~20 km-long studied river reach draining the north-western part of the footwall (Triffa plain) and the south-western part of the hanging wall (Ouled Mansour plateau, Fig. 2B). Geomorphological mapping was firstly based on DGPS (Topcon HiPer Pro) and laser distance meter (TruPulse 200 Rangefinder) measurements. Both were used to estimate the relative elevations of the main fluvial morphological landforms above the modern floodplain. Moreover, five valley cross sections in the hanging wall reach were obtained from DGPS elevation data (see location in Fig. 2B). The latter were corrected using the elevation of topographic points mentioned on Moroccan 1:50,000 topographic maps (Berkane, les Triffa and Zaio) and were processed with the *GPS-Track-Analyse.NET* software. DGPS and laser distance meter measurements reach an altimetric accuracy of ~2 cm and <0.3–0.5 m, respectively. To complement field mapping, Astrium satellite images provided by Google Earth were used: their resolution is appropriate for reconstructing the regional occurrence of major geomorphological units. They allowed inferring (i) the widths of both the present-day floodplain and the valley filled with Holocene overbank fines at twenty selected spots (see location in Fig. 2B), and (ii) the height of the fault scarp at the southern edge of the Ouled Mansour plateau along four cross sections (see location in Figs. 2A and B).

Two river profiles were thoroughly studied: the GAR and DOE profiles (Fig. 2B). They were selected because they are representative of the contrasting valley reaches draining the footwall and the hanging wall, respectively (see 4.2. and 4.3.). The ~37 m-high GAR profile is located on the western bank of the Moulouya (34°58'15.2" N; 2°27'35.7" O) and was measured by laser distance meter. The ~23 m-high DOE profile is located ~3.6 km downstream of the previous one, on the eastern bank of the Moulouya (34°59'59.2" N; 2°26'27.3" O) and was measured by laser distance meter and DGPS. Clast lithological analysis was applied to both profiles: two sets were collected in the lower and upper parts of the GAR profile and one in the DOE profile (see 4.2.2. and 4.3.2., respectively). For each set, more than 150 pebbles were directly extracted and sieved. Given the mean individual clast size in both profiles, analysis is

performed in the (very) coarse gravel fraction (–4 to –6 grain size classes on the ϕ scale, i.e. 1.6–6.4 mm). Clast lithological analysis performed in fluvial terraces is useful to unravel the source areas of coarse alluvial material transported by large rivers (e.g. Rixhon and Demoulin, 2010; Demir et al., 2012). Contrasting proportions observed in the clasts' nature may also reflect major catchment-wide changes in sediment supply (Maddy et al., 1991). At last, a quantitative evaluation of the carbonate content in the fine-grained matrix of the GAR profile was performed using the Scheibler apparatus, where 0.5 g of sediments was moistened and reacted with 10% HCl (Beck et al., 1993). Horizons of densely-cemented secondary carbonates frequently occur in ancient fluvial sediments of the Moulouya (Ruellan, 1971; Kaemmerer and Revel, 1991); this is typical for river terrace deposits of semi-arid Mediterranean environments (e.g. Candy and Black, 2009).

4. Geomorphological mapping and profile description

4.1. Lithological and morphological duality of the valley

Remarkable lithological variations associated with specific morphological features characterize the valley walls along the <1 km-long fault zone, located directly before the river cuts into the Ouled Mansour plateau (Figs. 2B and 3A). All observations detailed below are reported along flow direction: the footwall (Triffa plain) and the hanging wall (Ouled Mansour plateau) are the upstream and downstream reaches, respectively.

First, sharp lithological contacts are observed along the fault zone: the footwall reach is composed of fluvial gravels capped by fine-grained deposits, whereas the valley sides of the hanging wall reach are formed by marine sediments exhibiting different facies (Fig. 3A and B; see also sections 4.2 and 4.3). On the western valley side, the latter are composed of yellowish sands and greyish marls; they locally crop out in a 330 m-long and 190 m-wide landsliding area, located directly downstream of the lithological contact and stretching to the current channel (Fig. 3B). Note that these locally cemented sands and marls constitute most of both valley walls in the hanging wall further downstream. On the eastern valley side, light greyish fine-grained carbonate sediments containing abundant marine fossils (shell fragments mostly) form the hanging wall directly downstream of the lithological contact (Fig. 3C–E). Note that the latter is located >500 m southward of the lithological contact on the opposite valley side (Fig. 2B). Recrystallization processes associated with deep brownish/reddish colourations occur in these fossil-bearing sediments, both at depth and at the surface (Fig. 3C and D).

Second, clear vertical offsets disrupt the topography in the fault zone. While the vertical offset is 4–5 m-high on the western valley side (Fig. 3A), the fault scarp is very prominent on the opposite side and reaches heights up to 30–35 m eastward of the valley (Fig. 4). The scarp is (almost) continuously observable in the topography from the Moulouya valley (west) up to the valley of the Oued Kriss at the Algerian border (east) along more than 20 km (Fig. 2A). Note that its direction changes from WSW–ENE to W–E north of the locality of Madagh (Fig. 2A).

Third, larger-scale contrasts in the valley morphology and channel dynamics are readily recognizable in the several km-long reaches located up- and downstream of the fault zone. The valley geometry along with the elevation difference between the modern floodplain and the top of the valley walls is particularly contrasting: nearly symmetrical, 30–40 m-high valley walls evolve into asymmetrical ones, up to 50 and 90 m-high on the western and eastern river banks, respectively, directly downstream of the fault zone (Fig. 2B). The mean lateral development of the modern floodplain significantly increases from ~215 m to ~360 m between the footwall

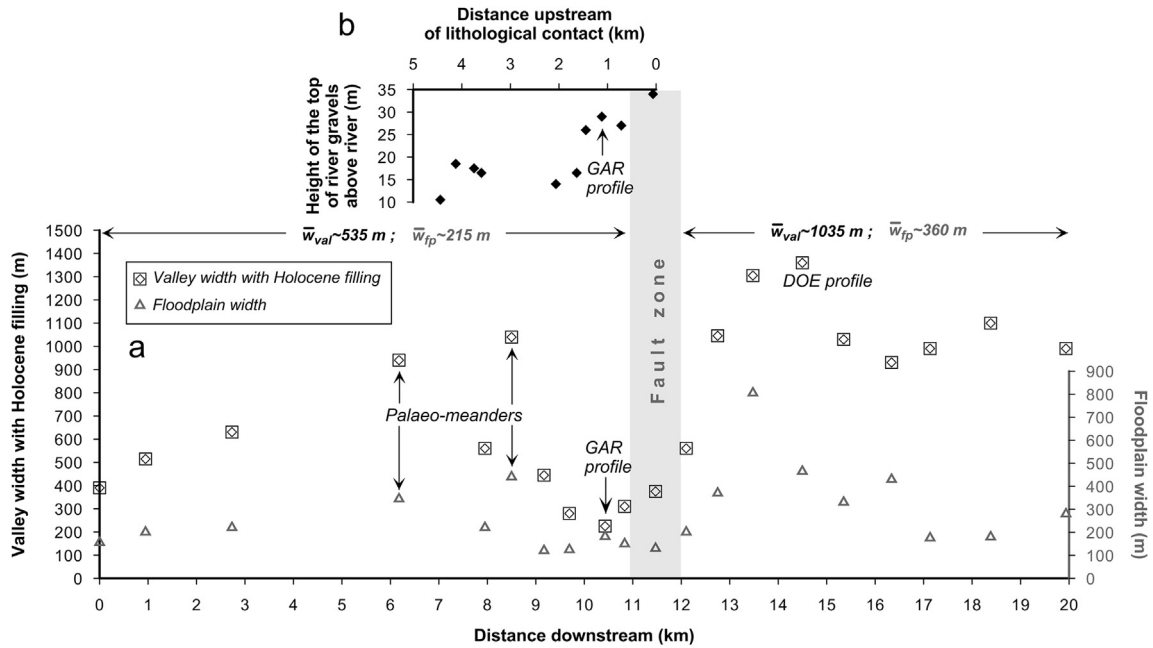


Fig. 5. (A) Evolution of the floodplain width and the valley width filled with Holocene flood deposits in the up- and downstream reaches of the fault zone (grey area), with location of the DOE and GAR profiles. Note the contrasting mean values between both valley reaches. (B) Elevation of the top of the cemented river gravel upstream of the lithological contact observed on the western valley side. This graph clearly reveals a diminishing trend in the upstream direction, decreasing from more than 30 m in the fault zone to about 10 m ca. 4 km upstream of it.

and the hanging wall (Fig. 5A). Whereas it is restricted to values below 180 m in the 2 km-long reach directly upstream of the fault zone, maximal values exceeding 800 m are observed only 1.5 km downstream of the fault zone. The mean valley width filled with Holocene overbank fines in the footwall is also twice as narrow as that of the hanging wall (~ 535 and ~ 1035 m, respectively, Fig. 5A). In particular, the valley width reaches minimal values of ~ 300 m in the 2 km-long reach directly upstream of the fault zone, whereas it rapidly exceeds 1000 m in the next kilometre downstream (Fig. 5A). At last, recent channel dynamics observed on satellite images (from 2003 to 2013) in the hanging wall is characterized both by incipient

free meandering in the broad floodplain and active point bar development and migration.

4.2. The footwall reach (Triffa plain)

4.2.1. General characteristics

Along the 10 km-long reach upstream of the fault zone, no Neogene marine sediment can be observed anywhere at the base of the valley walls. Here, the latter are formed by several m-thick cemented river gravels, capped by fine-grained sediments exhibiting several dm-thick calcretes at the top. These gravel bodies build

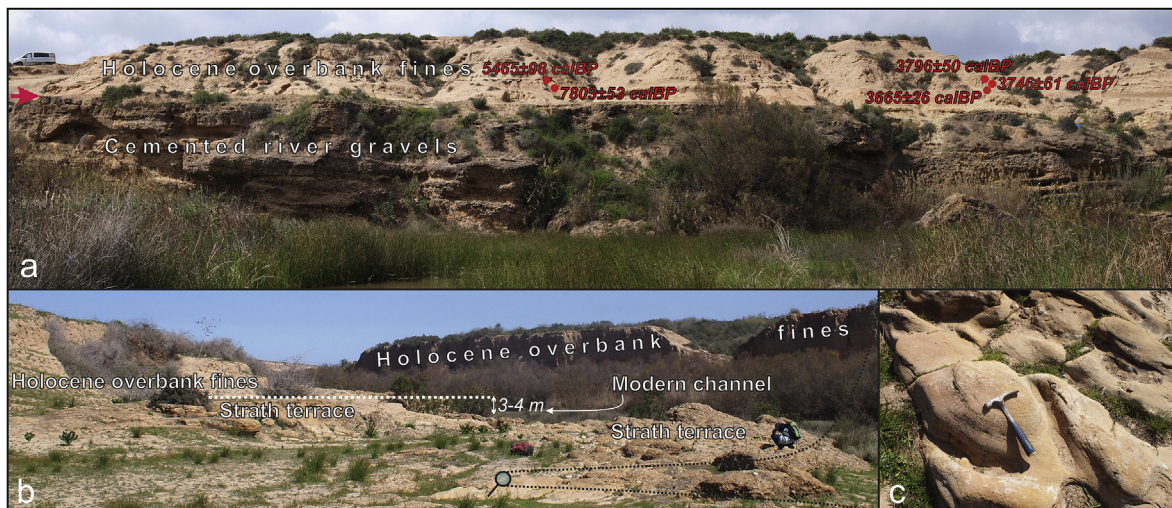


Fig. 6. (A) Panorama view of the outer bank of a meander located ~ 4 km upstream of the fault zone. Note the sharp contact (red arrow) between the underlying cemented Pleistocene river gravels and the overlying Holocene overbank fines, in which settlement sites of the Epipalaeolithic, Early Neolithic and Bronze age, attested by five ^{14}C dates (red circles), were found in archaeological excavations (Linstädter et al., 2012). (B) View of the strath terrace carved into cemented river gravels and sands, located ~ 2 km upstream of the fault zone. Also overlain by Holocene overbank fines, its top (white dashed line) is perched 3–4 m above the modern river channel. (C) Detailed view of the abrasion flutes and potholes observed on the strath surface. (All photos: G. Rixhon). (For interpretation of the references to colour in this figure legend, the reader is referred to the web version of this article.)

sub-vertical valley sides at several locations (see section 4.2.2). They frequently include cemented sand lenses, locally exhibiting cross-bedding. Holocene overbank fines are rarely present simultaneously on both river banks; they are discontinuous and frequently occur in the inner banks of meanders (Fig. 2B). Elevation measurements of the top of the river gravels above the current channel, where clearly identifiable, decrease from ~34 m in the fault zone to about 10 m ca. 4 km upstream of it (Fig. 5B). Recent overbank fines may locally overlie the cemented river gravels at locations where the observable gravel thickness does not exceed 10 m (Fig. 6A). ¹⁴C dating of former human settlement places embedded in these fine sediments attest a Holocene depositional age (Linsädter et al., 2012). A bench-like surface, located ~2 km upstream of the fault zone on the western valley side, is also observed. It is carved into cemented river gravels and sand lenses, displaying abrasion flutes and potholes (Fig. 6B and C). Partly covered by recent overbank fines, the top of this strath terrace is located 3–4 m above the current channel (Fig. 6B).

4.2.2. The GAR profile

The GAR profile is located on the western bank of the Moulouya, directly upstream of the fault zone (Fig. 2B). In this valley section, the narrow modern floodplain and the Holocene overbank fines (i.e. together less than 225 m-wide) are only observed on the eastern valley side whereas fluvial lateral erosion formed undercut slopes on the western valley side. The ~37 m-thick sedimentary succession of the profile exhibits a repetitive pattern of two similar fining-upward sequences: river gravel at the bottom (units 1 and 4), sand layers in the middle (units 2 and 5) and silty/clayey sediments at the top (units 3 and 6) in each sequence (Fig. 7A). The first sequence is at least ~23 m-thick (base not visible because of the water table) and the second is ~14 m-thick (Fig. 7A). Units 1 and 4, forming the lower and upper river gravel bodies, respectively, are ~15 and ~6 m-thick (depths of ~37–22 m and ~14–8 m). They are both clast-supported, poorly to moderately sorted and strongly cemented. Individual clast size usually amounts to several centimetres, rarely exceeding 20 cm. Both contain several m-long and dm-thick sand lenses, also cemented, that regularly display cross-bedding structures. CaCO₃ contents from the cemented fine-grained matrix amount to 53–70% in these units (Fig. 7B). Clast lithological analysis performed in each unit, however, reveals contrasting results (Fig. 7C). A dominance of carbonate rocks over rocks primarily built by silicate minerals is clearly observed in unit 1 (93 vs. 7%). This ratio between both rock types is much more balanced in unit 4: 52 vs. 48%. In unit 1, more than 50% of the analysed pebbles are microgranular limestone, sometimes with calcite veins, whilst other carbonates are macrogranular limestone/calcareous sandstone (21.2%), dolomite (11.3%), belong to other categories or are indeterminable, e.g. due to strong weathering (10%). Rocks built by silicate minerals, i.e. chert, sandstone, quartzite, slate and acidic volcanic rocks, are sparse. In unit 4, the same kinds of carbonate rocks are found but in lesser proportions: microgranular and macrogranular limestones amount to 34.2 and 7.5%, respectively, while dolomite only represents 7.0%. Rocks built by silicate minerals are much diverse but are primarily dominated by both high- and low-degree metamorphic rocks, amongst which quartzite, including quartz pebbles originating from neo-formed quartz veins (22.5%), and slate or phyllite (10.7%). Plutonic rocks, encompassing granitic, dioritic and sheet intrusion rocks, and basalt represent 5.9 and 3.2%, respectively. Chert pebbles amount to 3.2%; sandstone, grauwacke and breccia pebbles were also observed.

Units 2 and 5, forming the lower and upper cemented sand layers, respectively, are at least 3 m and several dm-thick (depths of ~22–19 m and ~8–7.5 m). They display, just like the sand lenses embedded in the gravel bodies, tafoni weathering features. CaCO₃ content amounts to 46–54% in these units (Fig. 7B). The (at least)

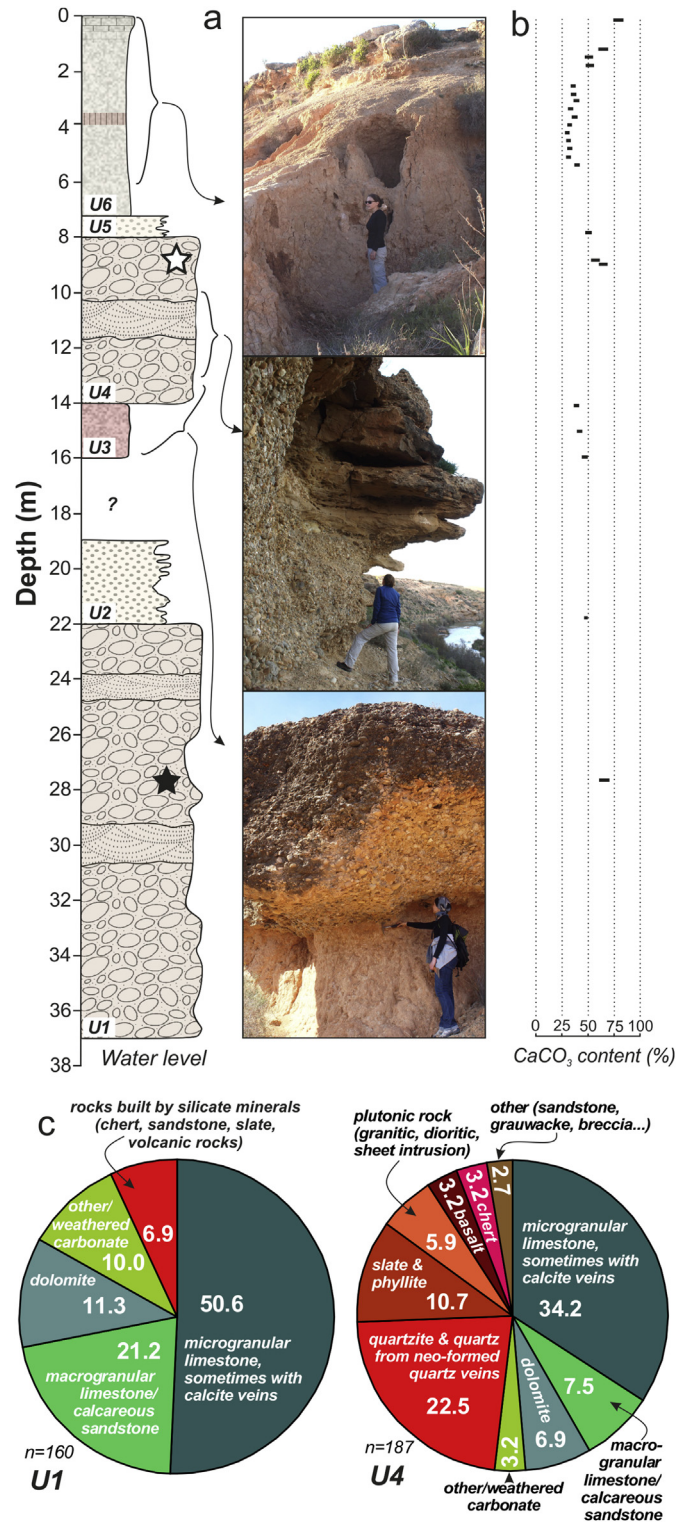


Fig. 7. (A) Stratigraphic log of the 37 m-thick GAR profile, illustrated by detailed photos, exhibiting a recurrent pattern of two similar fining-upward sequences: two stacked river terraces, each one built-up by a cemented river gravel body at the base and alluvium (floodplain loam) on top. U1 to U6 refer to the six sedimentary units (see 4.2.2.). The black and white stars represent the sampling locations for clast lithological analysis in the lower (U1) and upper (U4) gravel body, respectively. Top photo: overbank fines of U6; middle photo: cemented gravel body of U4, embedding a several dm-thick sand lens; bottom photo: sharp contact between the reddish silty/clayey sediments of U3 and the gravel body of U4 (the person points to the erosional discontinuity). (All photos: G. Rixhon). (B) Carbonate content in the fine-grained matrix. (C) Contrasting results of clast lithological analyses (numbers in percent).

2 m-thick cemented silty/clayey sediments forming unit 3 at depths comprised between ~16 and ~14 m are homogeneous and show a deep, uniform brownish/reddish colouration along with CaCO_3 contents ranging from 36 to 49% (Fig. 7B). While the lower contact of these sediments could not be identified, the upper contact with the overlying gravel body is sharp and erosive (Fig. 7A). The upper, light brownish, ~7–7.5 m-thick silty/clayey sediments forming unit 6 are homogeneous, although a several dm-thick layer characterized by a stronger reddish colouration is observable at mid-height. They also show a gradual upward induration, reflected by the CaCO_3 contents evolving from ~30% at the base to >75% at the top (Fig. 7B). The whole sequence is indeed sealed by a several dm-thick, very strongly cemented horizon.

4.3. The hanging wall reach (Ouled Mansour plateau)

4.3.1. General characteristics

In the several km-long reach downstream of the fault zone, thorough field survey together with DGPS measurements allowed to identify three distinct contacts between Neogene marine deposits and fluvial terrace sediments (Figs. 8 and 9), and to document their relative elevation above the modern floodplain. From the highest to the lowest, these contacts are found at relative elevations of 67 ± 1 , 35 ± 1 and 25 ± 1 m (Figs. 8 and 9), with associated absolute elevations of 77 ± 1 , 45 ± 1 and 35 ± 1 m above sea level. According to this, the corresponding terrace levels are named T1, T2 and T3, respectively (Figs. 8 and 9). They are characterized by an identical sedimentary pattern. Several m-thick, massive gravel bodies, strongly cemented due to the induration of the matrix material, are overlain by several m-thick fine-grained sediments, all sealed by a several dm-thick, locally dismantled calcrete (Fig. 8A and B). Frequent cemented sand lenses, locally exhibiting cross-bedding, are embedded in the gravel bodies. These cemented terrace sediments can be traced over several hundreds of meters in most instances; the corresponding terrace levels consequently build morphological units in the landscape (Fig. 8A). They are unequally distributed: T1 is only observable on the eastern valley side, T2 only on the western valley side and T3 on both of them (Fig. 2B). The nature of the underlying Neogene sediments also varies: locally cemented sands underneath T1 and T2, and marls underneath T3. Sand layers underlying T2 are strongly tilted to the west (Fig. 8C). Holocene overbank fines almost continuously occur on both river banks. Similarly to the older terrace levels, DGPS measurements reveal three main morphological units in the Holocene overbank fines with the following relative elevations above the current floodplain: 14 ± 2 , 6 ± 1 and 3 ± 1 m (Fig. 9). On the eastern valley side, a ~1.5 km-long palaeo-channel is cut into the Holocene 6 ± 1 m-high terrace (Fig. 9).

4.3.2. The DOE profile

It is located on the eastern bank of the Moulouya, more than one kilometre downstream of the fault zone (Fig. 2B). The base of the fluvial sediments unconformably lies on Neogene marls at a relative elevation of 25 ± 1 m (Fig. 10A) and allows for a correlation of these fluvial sediments to the T3 terrace. The contact could not be observed at the base of the DOE profile due to the presence of slope failure deposits, but it was clearly identified several hundred metres to the west of the profile. The overall ~22.5–23 m-thick profile is characterized by a fining-upward sequence (Fig. 10A): river gravel at the bottom (unit 1), sand body in the middle (unit 2) and silt/clay sediments at the top (unit 3). The up to 8–9 m-thick unit 1 corresponds to a massive, generally poorly-sorted and nearly completely cemented gravel body (depths from 23 to 15–14 m). A subdivision of unit 1 into three subunits with gradational contacts can be undertaken (Fig. 10B). The lowermost subunit is almost void of any organization and is characterized by the highest proportion of boulders, reaching up to 60 cm in size. The middle subunit shows large grain size variations from boulders (but less numerous than in the previous subunit) to sand, stratified in lenses. Clast orientation may locally be observed and several metre-long sand lenses sometimes exhibit cross-bedding structures (Fig. 10C). The uppermost subunit is clearly clast-supported due to the scarcity of the fine-grained matrix; in general it shows a better sorting of the pebble fraction. Lithological clast analysis reveals a clear predominance of carbonate rocks over rocks primarily built by silicate minerals (90.3 vs. 9.7%, respectively, Fig. 10D). As with the lower gravel body of the GAR profile, the same kinds of carbonate rocks are found, almost in identical proportions: microgranular limestone, sometimes including calcite veins, macrogranular limestone/calcareous sandstone and dolomite represent 51.9, 17.5 and 14.3%, respectively. The only significant difference concerns the composition of silicate rocks; only quartz (5.2%) and chert (4.5%) pebbles are found.

The sandy unit 2 cuts the underlying unit in a channel-like structure, implying thicknesses varying between ~4 and ~5 m (depths from 15–14 to 9.5–9 m, Fig. 10A). Where strongly cemented, it displays tafoni weathering features (Fig. 10B). It also includes channel structures filled with pebbles, one of them being several tens of metres-long but only a few decimetres-thick. The 9 to 9.5 m-thick unit 3 is formed of a homogeneous, light brownish silty/clayey stratum. In the upper part, it is characterized by a strong reddish colouration over a thickness of several metres (Fig. 10B). Although no carbonate content was measured in this profile, this unit also seems to exhibit a gradual upward cementation. Same as in the GAR profile, the whole sequence is sealed by a several dm-thick, very strongly cemented horizon.

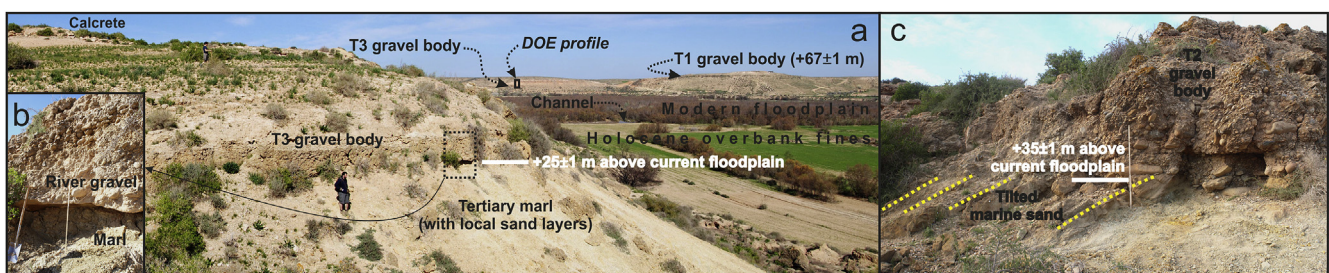


Fig. 8. (A) Panoramic view from the western valley side of the hanging wall reach and its terrace staircase incised into the Ouled Mansour plateau. In the foreground, sharp contact, i.e. erosional disconformity, between Neogene marl deposits and cemented river gravels of the terrace level T3, sealed by a calcrete (persons for scale). In the background, note the clear elevation difference between T3 and T1. The black rectangle refers to the DOE profile detailed in Fig. 10. Close-up of the erosional disconformity, stick is 1 m-long. (C) Sharp contact between Neogene sand deposits, partially lithified, and cemented river gravels of the terrace level T2 (stick is 1 m-long). Note the westward dipping (yellow dashed lines) of the sand layers. (Photos: M. Bartz and G. Rixhon). (For interpretation of the references to colour in this figure legend, the reader is referred to the web version of this article.)

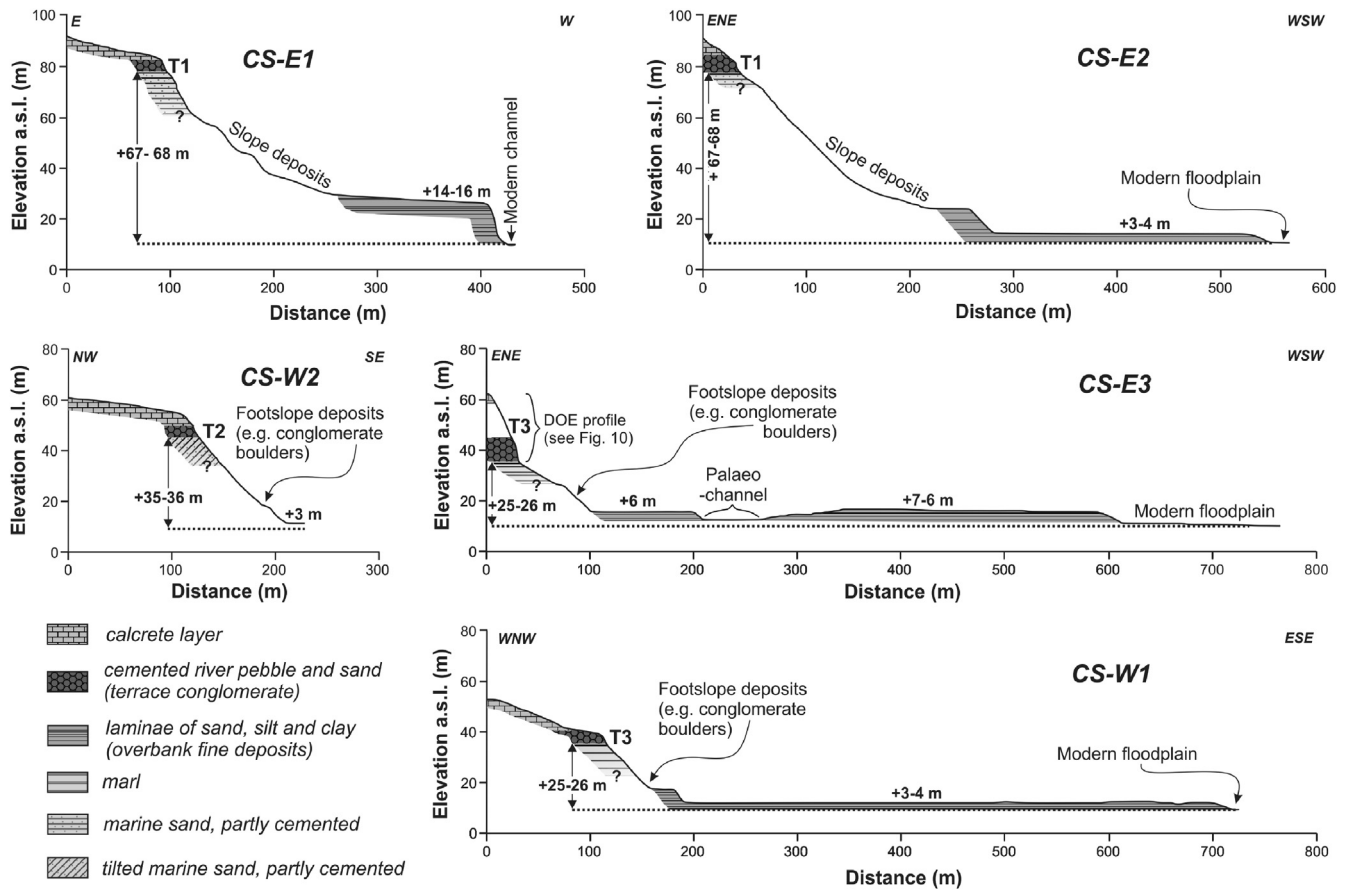


Fig. 9. Topographic cross sections based on DGPS measurements in the terrace staircase of the hanging wall reach (see Fig. 2B for location). Contacts between Neogene marine deposits and cemented river gravels at three distinct relative elevations above the current floodplain define three Pleistocene terrace levels, referred to as T1 to T3 from the highest to the lowest. Note also three other morphological units in the Holocene overbank fines (see 4.3.1.).

5. Data interpretation and discussion

The main thrust zone identified in this study (see section 5.3) has obviously affected the long-term evolution of the lower Moulouya. As attested by our field observations and data, fault activity lead to very much contrasting fluvial reactions up- and downstream of the thrust zone: fluvial aggradation primarily occurred in the footwall block (Triffa plain), whereas development of a terrace flight related to gradual river incision occurred in the uplifted hanging wall (Ouled Mansour plateau). Similar contrasting fluvial environments are indeed commonly observed where river systems cut across active thrust zones (e.g. Cording et al., 2014; Monegato and Poli, 2015), notably involving considerable deformations of terrace profiles (Thompson et al., 2002; Amos et al., 2007).

5.1. Stacked terraces and calcrete development in the footwall reach

The ~37 m-thick, fluvial sedimentary succession of the GAR profile points to long-lasting aggradation in the footwall reach. It also probably reveals a composite fill terrace (e.g. Pazzaglia, 2013), with a second terrace body (~14 m-thick) stacked over the first main one (at least ~23 m-thick). Arguments for this interpretation are (i) the recurring pattern of two similar fining-upward sequences, i.e. from gravel at the bottom to silt/clay at the top; (ii) the deep reddish colouration of the intermediate fines, indicating paleosol development in the middle of the sequence; (iii) the sharp erosive contact between intermediate fines (unit 3) and the upper gravel body (unit 4).

In the same profile, the different petrographic assemblages of both gravel bodies must also be discussed (Fig. 7C). The prevailing amount of carbonate rocks in the lower terrace body (>90%) probably reflects a local origin of the transported material, with predominant inputs from the Beni Snassen and/or the Kebbana mountains. Both massifs are primarily composed of diverse kinds of Mesozoic carbonates rocks (see 2.3.1.; Hollard, 1985). By contrast, the upper terrace body is characterized by a balanced proportion between carbonates rocks on the one hand and varied metamorphic (quartz/quartzite, slate, phyllite) and plutonic (granite, diorite, dyke-related) rocks as well as basalt on the other hand. With the exception of the small-sized batholith in the Beni Snassen massif, the second kind of rocks is practically absent in the lower Moulouya catchment. This points to a more complex mixing of the river bedload, reflecting both local input and longitudinal input from further upstream. In this respect, the largest outcrop of crystalline rocks is located in the upper Moulouya, directly upstream of the Ksabi basin (Fig. 1B; Hollard, 1985; Margoum et al., 2015). The main trunk, along a >50 km-long reach, and several tributaries have incised into both plutonic rocks (granite, granodiorite, diorite), belonging to the Paleozoic Aouli batholith, and associated contact metamorphic rocks (quartzite, micaceous schist). Triassic basalt occurs in this area as well and in the lowermost part of the Za catchment (Hollard, 1985; Margoum et al., 2015), the main eastern tributary of the Moulouya (Fig. 1A). Granitic rocks also crop out in this second area but to a much lesser extent than in the upper Moulouya and metamorphic rocks are almost absent there (Hollard, 1985). Since the latter represent more

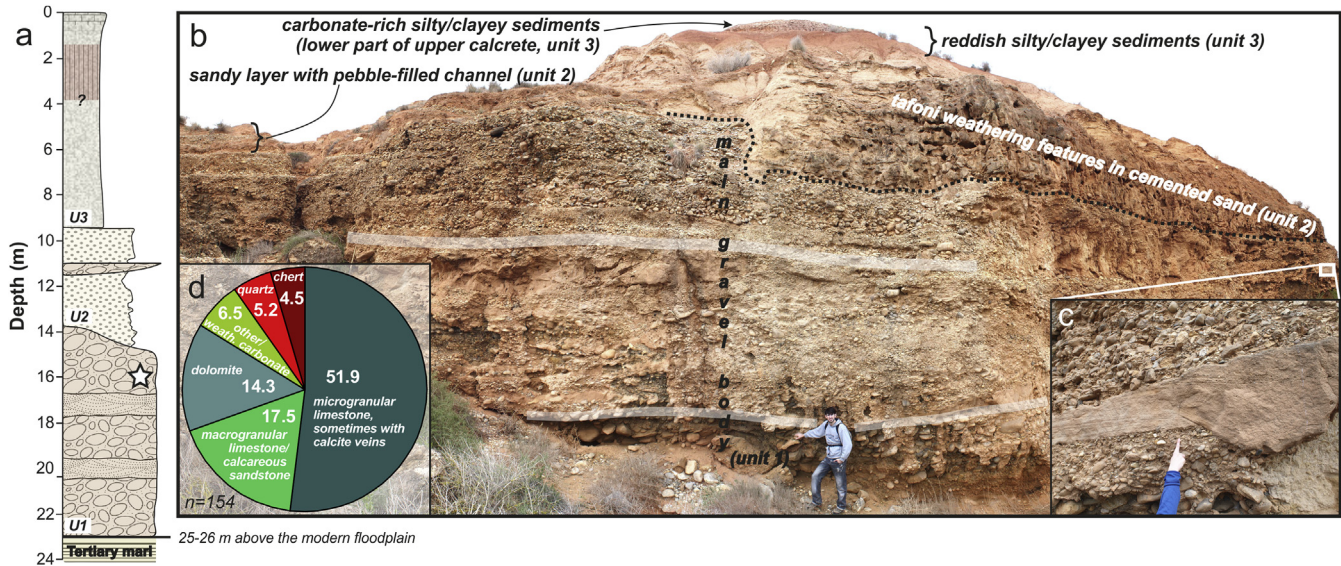


Fig. 10. (A) Stratigraphic log of the 22–23 m-thick DOE profile, exhibiting a fining-upward sequence with three distinct units (U1 to U3). The white star refers to the sampling location for clast lithological analysis. (B) Panoramic view of the profile, showing the main gravel body (U1) and the overlying sandy (U2) and silty/clayey (U3) sediments. The dashed black line delimits the boundary between U1 and U2. The white stripes refer to the transition zones between the different sub-units of U1 (see 4.3.2.). The white rectangle refers to Fig. 10C. (C) Detailed view of a sand lens embedded in U1 and exhibiting cross-bedding. (D) Result of clast lithological analysis (numbers in percent). (All photos: G. Rixhon).

than 30% of the clasts analysed in unit 4 of the GAR profile (Fig. 7C), we assume that material eroded from the upper Moulouya area was significantly deposited in the upper terrace body. We thus suggest that such a petrographic variation in the transported bedload might reflect an important catchment-wide change in sediment supply (Maddy et al., 1991): deeper basement rocks have been probably unroofed and denudated in this erosional area and transported up to the lower Moulouya sedimentary basin located several hundreds of kilometres downstream. This change in sediment supply might have been related to the transition of the Ksabi-Missouri basin from an endorheic to an exorheic drainage system as a result of its capture by a former Moulouya river (Pastor et al., 2015). It remains however unknown when this piracy event occurred after the last depositional episode in this basin during the Early Pliocene (Pastor et al., 2015). We finally argue that the observed petrographic change is an additional argument for long-lasting, perhaps discontinuous, aggradation in the footwall reach, leading to the formation of a composite fill terrace, i.e. the deposition of these crystalline rocks occurred after the formation of the lower terrace body.

We also observe a bipartite distribution of carbonate contents in the matrix of the GAR profile: it displays relatively high values from unit 1 to unit 5 and a decrease at the base of unit 6 followed by a significant upward increase (Fig. 7B). We suggest that different processes were involved in secondary carbonate precipitation and calcrete formation. Sealing the sediment sequence, the very upper part probably corresponds to a densely-cemented hardpan horizon (Kaemmerer and Revel, 1991; Candy and Black, 2009). Very frequently encountered in semi-arid Mediterranean environments, it is typical of *per descendum* calcrete profiles and is associated to pedogenic processes (Ruellan, 1971; Kaemmerer and Revel, 1991; Candy and Black, 2009). In contrast, the rather homogeneous cementation in the lower part of the sequence is probably the result of processes resumed under the generic term of groundwater calcrete (Kaemmerer and Revel, 1991; Candy and Black, 2009). More specifically, it might correspond either to a channel calcrete (Nash and Smith, 2003) or more likely to a valley calcrete (Nash and McLaren, 2003); the latter is typically several m-thick and

develops within broad drainage courses, cementing alluvium of valley flanks. We assume that the same general bipartite interpretation can be drawn for fluvial sediments of the lower Moulouya where a similar cementation pattern is observed (e.g. in the DOE profile). In the Ksabi basin (Fig. 1A), the same conclusion was reached by Kaemmerer and Revel (1991), who also identified a bipartite induration pattern in old terrace sediments of the Moulouya. However, further investigations, including micromorphology (Nash and McLaren, 2003), are required to better specify calcium carbonate accumulation and calcrete formation in our study area.

5.2. Pleistocene terrace staircase and related incision episodes in the hanging wall reach

The Moulouya developed a well-preserved terrace flight with three distinct terrace levels in the hanging wall reach: they are named T1 to T3, from the highest to the lowest (Figs. 8, 9). Their strongly cemented gravel deposits, due to massive secondary CaCO_3 precipitation (see 4.2.2.), contrast with the loose gravel and the unconsolidated clayey/silty/sandy laminae forming the current channel and the Holocene overbank fines, respectively. T1, T2 and T3 are thus interpreted as Pleistocene terrace deposits. A similar conclusion was reached by Ruellan (1971): latest Pleistocene and Holocene deposits in the Zebra and Triffa plains bear (almost) no traces of any carbonate redistribution, whereas older Pleistocene deposits are all cemented by carbonate precipitation. Sedimentary successions from the three Pleistocene terrace levels, though only clearly exposed for T3, seem also to display fining-upward sequences, just like in the aggradation area of the footwall reach. These observations converge with the terrace stratigraphy in the Ksabi basin (Fig. 1A). A similar sedimentary pattern was recognized in all of the 10–15 m-thick alluvial formations there (Lefevre, 1989); it consists of (i) an erosional contact at the base; (ii) a bipartite conglomerate, i.e. heterometric, boulder-rich and unstratified in the lower part evolving into metre-sized oblique and cross-bedded layering to the top; (iii) solidified sands with oblique bedding; and (iv) laminated silty layers capping the sequence (where still present). This sequence is remarkably similar to the one exhibited in

the DOE profile (Fig. 10). We therefore assume that there is a recurrent fining-upward sequence in Pleistocene terrace deposits along the whole Moulouya course. We agree with Lefèvre's (1989) correlation between the deposition of the coarse sediment layers and river systems of high competence, characterized by former torrential flow regimes. This is particularly well exemplified by the lowermost subunit in the DOE profile, with no sedimentary organization and the highest proportion of boulders up to 60 cm in size (Fig. 10B). Such a depositional environment is usually encountered in semi-arid streams significantly affected by flash floods and characterized by high sediment supplies (Thorndycraft and Benito, 2006).

Incised into the underlying Neogene marine sediments, the terrace staircase in the hanging wall thereby records three main Pleistocene downcutting episodes after the formation of T1 (Fig. 11). From the top to the base, they amount to slightly more than 30 m, ~10 m and >25 m, based on the vertical spacing between the bases of successive terrace levels, and in the third case, between T3 and the unrecognized base of the current floodplain. According to Pazzaglia (2013), given the alluvium thickness of each Pleistocene terrace level (see Fig. 9), they are all likely to represent fill terraces (Fig. 11), exhibiting clear erosive contacts at their respective bases (Fig. 8).

Interpreting the three morphological units in the Holocene overbank fines, observable on both sides of the fault zone, is more delicate. They may correspond either to a main ~15–16 m-thick aggradational terrace subsequently cut by two degradational terraces at relative elevations of 6 ± 1 and 3 ± 1 m (Fig. 11), or to three distinct aggradational terraces. In the main aggradational terrace, the ^{14}C age distribution in the different profiles investigated by Zielhofer et al. (2008, 2010, see Fig. 2b) repeatedly and consistently displays younger deposition ages from the base to the top: the most recent age of ~1.4 ka is found at a relative elevation of ~14 m. This age distribution and the strath terrace carved in older fluvial deposits at a relative elevation of 3 ± 1 m (Fig. 6B) both argue for the first interpretation. A similar conclusion was reached by Pissart and Boumeaza (2010).

5.3. Identification of a main thrust zone in north-eastern Morocco

5.3.1. Implications at the basin scale

Previous studies interpreted either the southern edge of the Ouled Mansour plateau as a major flexure (Ruellan, 1971; Boughriba et al., 2006; Fetouani et al., 2008) or the whole structure as a Miocene horst, implying the presence of normal faults at its borders (Khattach et al., 2004; Chennouf et al., 2007a). On the one hand, we reject the hypothesis of a flexure in the very upper part of the Earth's crust in the light of our new observations and

data, i.e. sharp and anomalous lithological contacts, recrystallization processes and diverse morphological variations including contrasting fluvial environments within a very short distance. On the other hand, faulting is much more adequate to explain our observations. This agrees well with recent studies using gravimetric and aeromagnetic data: the location of the >20 km-long continuous fault scarp indeed fairly well matches W–E to WSW–ENE striking lineaments independently detected in this area (Khattach et al., 2006; Chennouf et al., 2007b; El Gout et al., 2010). However, the hypothesis of a horst structure must be questioned against the geodynamic background of north-eastern Morocco (Khattach et al., 2004; Chennouf et al., 2007a). Normal faults accommodate extensional stress in the Earth's crust (e.g. Twiss and Moores, 2007) and this contradicts the widely recognized N–S compressive shortening having occurred since the Late Neogene in this region (Meghraoui et al., 1996; Ait Brahim et al., 2002; Fadil et al., 2006; Vernant et al., 2010; Barcos et al., 2014). Moreover, gravimetric-induced observations (Khattach et al., 2006; Chennouf et al., 2007b; El Gout et al., 2010) highlight a NNW dip of the WSW–ENE striking fault segment matching the ~10 km-long fault scarp between the Moulouya valley to the west and the locality of Madagh to the east (Fig. 2A). Although fault motion is not indicated, the fault geometry and the higher topographic position of the Ouled Mansour plateau imply that the latter was the upthrown hanging wall block. In the light of these new considerations, we interpret this structure as a thrust zone disrupting the lowermost sedimentary basin of the Moulouya.

Lithological contacts observed along both valley sides of the Moulouya are also slightly shifted (Fig. 2B). On the eastern valley side, the ~500 m-long offset to the south might be related to a subsidiary splay fault branching off from the main thrust (Twiss and Moores, 2007). Folding of the Neogene marine layers seems also associated to thrusting motion, as pointed out by the westward dipping of the partly solidified sand layers underneath the T2 terrace (Fig. 8C). Finally, the identification of this thrust zone in this sedimentary basin surely has implications on the local aquifer structure and water resources in the Triffa plain and Ouled Mansour plateau. This possibly implies a re-examination of several interpretations drawn by recent studies, which formerly interpreted the southern edge of the Ouled Mansour plateau as a large flexural feature (Boughriba et al., 2006; Fetouani et al., 2008).

5.3.2. Regional implications

The presence of this large thrust zone in the lowermost sedimentary basin of the Moulouya must also be discussed at a regional scale. First, it validates the assumption of the W–E striking main deformational front between the Rif belt and the Atlas mountains in the north-eastern part of Morocco (Barcos et al., 2014). This thrust zone is consistent with the statement that a substantial part of the N–S compressive shortening was accommodated along reverse faults located at the northern margins of the Beni Snassen massif and the Kbdana mountains (Barcos et al., 2014). A similar conclusion was previously reached by El Gout et al. (2010). Our observations clearly demonstrate that the studied thrust zone has accommodated a part of this deformation. Contrary to the claim that the marine/continental sediment cover of the Neogene-Quaternary impedes the recognition of fault patterns in the sedimentary basins of north-eastern Morocco (Chennouf et al., 2007b), we state that recent faulting activity in these basins significantly deformed the Neogene and Quaternary sediments and left clear imprints in the topography.

Second, morphometric indicators along with deformations of the drainage in the Moulouya catchment point to a general disequilibrium state (Barcos et al., 2014; Pastor et al., 2015). In particular, two major knickzones are conspicuous in the

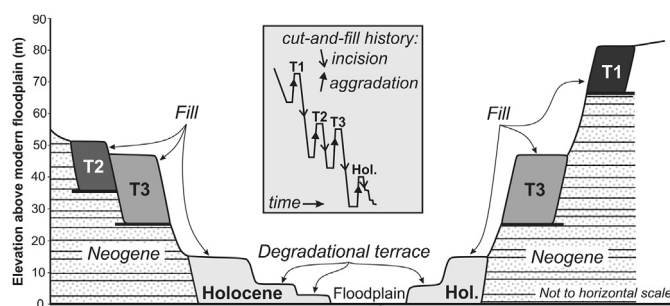


Fig. 11. Schematic sketch of the terrace staircase in the hanging wall reach, differentiating fill terraces from degradational terraces (bold black lines refer to the base of the Pleistocene terraces observed in the field). Multiple cut-and-fill events are outlined in the grey box.

longitudinal profile (Fig. 1B). While the upstream knickzone corresponds to the deeply-incised reach into the crystalline rocks of the Palaeozoic Aouli batholith (and related metamorphic rocks), the downstream one occurs in the Mesozoic limestones of the Beni Snassen gorge. According to Pastor et al. (2015), the upstream knickzone is related to the capture of the Ksabi-Missour basin (located downstream, see Fig. 1A), which occurred at an unknown time period after the Early Pliocene (see section 5.1). This capture induced the upstream propagation of an erosion wave which, when reaching the resistant crystalline rocks at the basin margin, resulted in the formation of a lithological knickzone. Bouazza et al. (2009) similarly suggested that the formation of the Beni Snassen gorge and the related knickzone resulted from several capture episodes at the onset of the Quaternary, although these authors provided no clear evidence for this explanation. Alternatively, it is well known that surface rupture resulting from fault motion often create knickpoints in the river channel and that these retreat at varying rates along the drainage network (e.g. Whittaker and Boulton, 2012; Cook et al., 2013; Boulton et al., 2014). Without explicitly rejecting the capture hypothesis, we suggest that the 30 km-long knickzone in the Beni Snassen gorge could also (partly) result from a transient fluvial reaction to Quaternary thrusting activity in the sedimentary basin and correlated uplift in the hanging wall block which is located >35 km downstream of the gorge outlet. In this respect, Boulton et al. (2014) showed that knickpoint formation in the Dades catchment (High Atlas) was related to increased Plio-Quaternary uplift rates as a result of fault activity along a main thrust zone (i.e. South Atlas Fault).

6. Conclusion and further research perspective

Our study confirms the usefulness of the terrace record of large rivers to investigate long-term crustal deformation. Significant thrusting activity in the lowermost sedimentary basin of the Moulouya, associated with N–S compressive shortening in this region, led to contrasting fluvial reactions and environments. On the one hand, long-lasting fluvial aggradation, materialized by 37 m-thick stacked terraces, has occurred in the footwall of the thrust. On the other hand, the hanging wall is characterized by a well-preserved terrace staircase, with (at least) three Pleistocene terrace levels. Late Cenozoic deformation and uplift induced in the hanging wall probably hindered profile regularisation of the Moulouya and might have been responsible for the knickzone observed in the Beni Snassen gorge. These interpretations agree well with independent morphometric indicators highlighting the disequilibrium state of the whole Moulouya catchment. Moreover, we showed that stratigraphies of Pleistocene terrace deposits display similar sequences in the middle and lower reaches of the river.

Assessing the rates of crustal deformation along this main thrust zone related to the ongoing collision between the African and Eurasian plates obviously constitutes the next decisive step; it therefore requires age estimations for these Pleistocene terrace deposits of the lower Moulouya. As recently stated by Rixhon et al. (2016), luminescence (OSL/IRSL) and electron spin resonance (ESR) dating techniques form one array of potentially applicable methods for the considered time span. In a northern tributary system of the Moulouya catchment, first OSL age estimates obtained on Late Pleistocene and Holocene wadi deposits highlighted the suitability of this method (Bartz et al., 2015). Likewise, the presence of quartz or quartz-bearing pebbles in the investigated profiles would allow for the application of cosmogenic nuclide dating (^{10}Be and ^{26}Al). In this case, burial dating, especially isochron dating, would be more favourable and/or suitable than surface exposure dating because of the significant thickness of silty/clayey deposits capping the terrace

gravels.

Acknowledgements

This study was part of our research project C2 under the umbrella of the CRC 806 “Our Way to Europe”, funded by the German Research Foundation (DFG) (ref. no. SFB 806/2). We warmly thank Aurelia Hubert-Ferrari and an anonymous reviewer; their insightful and pertinent comments greatly help improving the quality of this manuscript. We also thank the students for their enthusiastic support during the field campaign and Rolf Hollerbach (University of Cologne) for his kind assistance for the clast lithological analysis.

References

- Ait Brahim, L.A., Chotin, P., Hinaj, S., Abdelouafi, A., Adraoui, A., El, 2002. Paleostress evolution in the Moroccan African margin from Triassic to present. *Tectonophysics* 357, 187–205.
- Akoglu, A.M., Cakir, Z., Meghraoui, M., Belabbes, S., El Alami, S.O., Ergintav, S., Akyüz, H.S., 2006. The 1994–2004 Al Hoceima (Morocco) earthquake sequence: conjugate fault ruptures deduced from InSAR. *Earth Planet. Sci. Lett.* 252, 467–480.
- Amos, C.B., Burbank, D.W., Nobes, D.C., Read, S.A.L., 2007. Geomorphic constraints on listric thrust faulting: implications for active deformation in the Mackenzie Basin, South Island, New Zealand. *J. Geophys. Res. Solid Earth* 112, 1–24.
- Babault, J., Teixell, A., Arboleya, M.L., Charroud, M., 2008. A late Cenozoic age for long-wavelength surface uplift of the Atlas Mountains of Morocco. *Terra Nov.* 20, 102–107.
- Barcos, L., Jabaloy, A., Azdimousa, A., Asebriy, L., Gómez-Ortiz, D., Rodríguez-Peces, M.J., Tejero, R., Pérez-Peña, J.V., 2014. Study of relief changes related to active doming in the eastern Moroccan Rif (Morocco) using geomorphological indices. *J. Afr. Earth Sci.* 100, 493–509.
- Bartz, M., Klasen, N., Zander, A., Brill, D., Rixhon, G., Seeliger, M., Eiwanger, J., Weniger, G.-C., Mikdad, A., Brückner, H., 2015. Luminescence dating of ephemeral stream deposits around the Palaeolithic site of Ifri n'Ammar (Morocco). *Quat. Geochronol.* 30, 460–465.
- Beck, S., Burger, D., Pfeffer, K.-H., 1993. Laborskript, Kleinere Arbeiten aus dem Geographischen Institut der Universität Tübingen, p. 11.
- Bouazza, A., Ait Brahim, L., Dugué, O., Laville, E., Delcaillau, B., Cattaneo, G., Charroud, M., de Luca, P., 2009. Changements Sédimentaires dans les Bassins Néogènes de Taourirt et Guercif (Maroc Oriental): recherche de l'épisode d'érosion Messinienne. *Eur. J. Sci. Res.* 28, 317–327.
- Boughriba, M., Melloul, A., Zarhloule, Y., Ouadi, A., 2006. Extension spatiale de la salinisation des ressources en eau et modèle conceptuel des sources salées dans la plaine des Triffa (Maroc nord-oriental). *Comptes Rendus Geosci.* 338, 768–774.
- Boulton, S.J., Stokes, M., Mather, A.E., 2014. Transient fluvial incision as an indicator of active faulting and Plio-Quaternary uplift of the Moroccan high Atlas. *Tectonophysics* 633, 16–33.
- Candy, I., Black, S., 2009. The timing of Quaternary calcrete development in semi-arid southeast Spain: investigating the role of climate on calcrete genesis. *Sediment. Geol.* 220, 6–15.
- Chennouf, T., Khattach, D., Milhi, A., Andrieux, P., Keating, P., 2007a. Détermination de la structure du bassin des Triffa par interprétation conjointe des données gravimétriques et sismiques : implications hydrogéologiques. *Geomaghreb* 4, 15–20.
- Chennouf, T., Khattach, D., Milhi, A., Andrieux, P., Keating, P., 2007b. Principales lignes structurales du Maroc nord-oriental : apport de la gravimétrie. *Comptes Rendus Geosci.* 339, 383–395.
- Cook, K.L., Turowski, J.M., Hovius, N., 2013. A demonstration of the importance of bedload transport for fluvial bedrock erosion and knickpoint propagation. *Earth Surf. Process. Landforms* 38, 683–695.
- Cording, A., Hetzel, R., Kober, M., Kley, J., 2014. 10Be exposure dating of river terraces at the southern mountain front of the Dzungarian Alatau (SE Kazakhstan) reveals rate of thrust faulting over the past ~400ka. *Quat. Res.* 81, 168–178.
- Demir, T., Seyrek, A., Westaway, R., Guillou, H., Scaillet, S., Beck, A., Bridgland, D.R., 2012. Late Cenozoic regional uplift and localised crustal deformation within the northern Arabian Platform in southeast Turkey: investigation of the Euphrates terrace staircase using multidisciplinary techniques. *Geomorphology* 165–166, 7–24.
- El Gout, R., Khattach, D., Houari, M.-R., Kaufmann, O., Aqil, H., 2010. Main structural lineaments of north-eastern Morocco derived from gravity and aeromagnetic data. *J. Afr. Earth Sci.* 58, 255–271.
- Fadil, A., Vernant, P., McClusky, S., Reilinger, R., Gomez, F., Ben Sari, D., Mourabit, T., Feigl, K., Barazangi, M., 2006. Active tectonics of the western Mediterranean: geodetic evidence for rollback of a delaminated subcontinental lithospheric slab beneath the Rif Mountains, Morocco. *Geology* 34, 529–532.
- Faure-Muret, A., Morel, J.-L., 1994. Carte néotectonique du Maroc, Feuille 1 : Provinces du Nord, échelle : 1/1 000 000. Edition du Service Géologique du Maroc. Ministère de l'Énergie et des Mines, Rabat.

- Fetouani, S., Sbaa, M., Vanclooster, M., Bendra, B., 2008. Assessing ground water quality in the irrigated plain of Triffa (north-east Morocco). *Agric. Water Manag.* 95, 133–142.
- Hollard, H., 1985. Carte géologique du Maroc (échelle 1/1 000 000). Edition du Service Géologique du Maroc. Ministère de l'Énergie et des Mines, Rabat.
- Ibouhouten, H., Zielhofer, C., Mahjoubi, R., Kamel, S., Linstädter, J., Mikdad, A., Bussmann, J., Werner, P., Härtling, J.W., 2010. Archives alluviales holocènes et occupation humaine en Basse Moulouya (Maroc nord-oriental). *Géomorphologie Relief, Process. Environ.* 1, 41–56.
- Kaemmerer, M., Revel, J.C., 1991. Calcium carbonate accumulation in deep strata and calcrete in quaternary alluvial formations of Morocco. *Geoderma* 48, 43–57.
- Khattach, D., Keating, P., Mili, E.M., Chennouf, T., Andrieux, P., Milhi, A., 2004. Apport de la gravimétrie à l'étude de la structure du bassin des Triffa (Maroc nord-oriental): implications hydrogéologiques. *Comptes Rendus Geosci.* 336, 1427–1432.
- Khattach, D., Miraoui, H., Sbibih, D., Chennouf, T., 2006. Analyse multi-échelle par ondelettes des contacts géologiques: application à la carte gravimétrique du Maroc nord-oriental. *Comptes-Rendus Geosci.* 338, 521–526.
- Lefèvre, D., 1984. Nouvelles données sur l'évolution plio-pléistocène du bassin de Ksabi (Moyenne Moulouya, Maroc). *Comptes-Rendus Académie Sci. Paris* 299, 1411–1415.
- Lefèvre, D., 1989. Formations continentales pléistocènes et paléoenvironnements sédimentaires dans le bassin de Ksabi (Moyenne Moulouya, Maroc). *Bull. Assoc. fr. étude Quat.* 26, 101–113.
- Linstädter, J., Aschrafi, M., Ibouhouten, H., Zielhofer, C., Bussmann, J., Deckers, K., Müller-Sigmund, H., Hutterer, R., 2012. Flussarchäologie der Moulouya-Hochflutebene, NO-Marokko. *Madr. Mittl.* 53, 1–84.
- Maddy, D., Keen, D.H., Bridgland, D.R., Green, C.P., 1991. A revised model for the Pleistocene development of the River Avon, Warwickshire. *J. Geol. Soc., Lond.* 148, 473–484.
- Margoum, D., Bouabdellah, M., Klügel, A., Banks, D.A., Castorina, F., Cuney, M., Jébrak, M., Bozkaya, G., 2015. Pangea rifting and onward pre-Central Atlantic opening as the main ore-forming processes for the genesis of the Aouli REE-rich fluorite-barite vein system, Upper Moulouya District, Morocco. *J. Afr. Earth Sci.* 108, 22–39.
- Meghraoui, M., Morel, J.-L., Andrieux, J., Dahmani, M., 1996. Tectonique plio-quaternaire de la chaîne tello-riffaine et de la mer d'Alboran. Une zone complexe de convergence continent-continent. *Bull. Soc. Geol. Fr.* 167, 141–157.
- Monegato, G., Poli, M.E., 2015. Tectonic and climatic inferences from the terrace staircase in the Meduna valley, eastern Southern Alps, NE Italy. *Quat. Res.* 83, 229–242.
- Nash, D.J., McLaren, S.J., 2003. Kalahari valley calcretes: their nature, origins, and environmental significance. *Quat. Int.* 111, 3–22.
- Nash, D.J., Smith, R.F., 2003. Properties and development of channel calcretes in a mountain catchment, Tabernas Basin, southeast Spain. *Geomorphology* 50, 227–250.
- Pastor, A., Babault, J., Owen, L.A., Teixell, A., Arboleya, M.-L., 2015. Extracting dynamic topography from river profiles and cosmogenic nuclide geochronology in the Middle Atlas and the High Plateaus of Morocco. *Tectonophysics* 663, 95–109.
- Pazzaglia, F.J., 2013. Fluvial terraces. In: Shroder, J., Wohl, E. (Eds.), *Treatise on Geomorphology, Fluvial Geomorphology*, vol. 9. Academic Press, San Diego, CA, pp. 379–412.
- Pissart, A., Boumeaza, T., 2010. Âge et origine de la terrasse limoneuse de la basse-Moulouya (Maroc nord-oriental). *Bull. Société Géogr. Liège* 54, 85–96.
- Poujol, A., Ritz, J.-F., Tahayt, A., Vernant, P., Condomines, M., Blard, P.-H., Billant, J., Vacher, L., Tibari, B., Hni, L., Idrissi, A.K., 2014. Active tectonics of the Northern Rif (Morocco) from geomorphic and geochronological data. *J. Geodyn.* 77, 70–88.
- Raynal, R., 1961. Plaines et piedmonts du bassin de la Moulouya. *Etude géomorphologique*. Rabat 617.
- Rixhon, G., Demoulin, A., 2010. Fluvial terraces of the Amblève: a marker of the Quaternary river incision in the NE Ardennes massif (Western Europe). *Z. für Geomorphol.* 54, 161–180.
- Rixhon, G., Briant, R.M., Cordier, S., Duval, M., Jones, A., Scholz, D., 2016. Revealing the pace of river landscape evolution during the Quaternary: recent developments in numerical dating methods. *Quat. Sci. Rev.* <http://dx.doi.org/10.1016/j.quascirev.2016.08.016> (in press).
- Rouchy, J.M., Pierre, C., Et-Touhami, M., Kerzazi, K., Caruso, A., Blanc-Valleron, M.M., 2003. Late Messinian to early Pliocene paleoenvironmental changes in the Melilla basin (NE Morocco) and their relation to Mediterranean evolution. *Sediment. Geol.* 163, 1–27.
- Ruellan, A., 1971. Contribution à la connaissance des sols des régions méditerranéennes: les sols à profil calcaire différencié des plaines de la basse Moulouya (Maroc oriental). *Mémoire Off. Rech. Sci. Tech. Outre-Mer*, p. 302.
- Sardinha, J., Carneiro, J.F., Zarhloule, Y., Barkaoui, A., Correia, A., Boughriba, M., Rimi, A., El Houadi, B., 2012. Structural and hydrogeological features of a Lias carbonate aquifer in the Triffa Plain, NE Morocco. *J. Afr. Earth Sci.* 73–74, 24–32.
- Snoussi, M., Haida, S., Imassi, S., 2002. Effects of the construction of dams on the water and sediment fluxes of the Moulouya and the Sebou rivers, Morocco. *Reg. Environ. Chang.* 3, 5–12.
- Thompson, S.C., Weldon, R.J., Berger, G.W., 2002. Late quaternary slip rates across the central Tien Shan, Kyrgyzstan, central Asia. *J. Geophys. Res.* 107 (B9), 2203.
- Thorndycraft, V.R., Benito, G., 2006. The Holocene fluvial chronology of Spain: evidence from a newly compiled radiocarbon database. *Quat. Sci. Rev.* 25, 223–234.
- Twiss, R.J., Moores, E.M., 2007. *Structural Geology*, second ed. W.H. Freeman and Company, New-York, p. 736.
- Vernant, P., Fadil, A., Mourabit, T., Ouazar, D., Koulali, A., Davila, J.M., Garate, J., McClusky, S., Reilinger, R., 2010. Geodetic constraints on active tectonics of the Western Mediterranean: implications for the kinematics and dynamics of the Nubia-Eurasia plate boundary zone. *J. Geodyn.* 49, 123–129.
- Whittaker, A.C., Boulton, S.J., 2012. Tectonic and climatic controls on knickpoint retreat rates and landscape response times. *J. Geophys. Res. Earth Surf.* 117, 1–19.
- Zarki, H., Macaire, J.-J., Beck, C., De Luca, P., 2004. Morphosedimentary evolution of the lower Moulouya (north eastern Morocco) during the middle and upper Holocene. *Seismicity Neotect. Eff. Geodin. Acta* 17, 205–217.
- Zielhofer, C., Bussmann, J., Ibouhouten, H., Fenech, K., 2010. Flood frequencies reveal Holocene rapid climate changes (Lower Moulouya River, northeastern Morocco). *J. Quat. Sci.* 25, 700–714.
- Zielhofer, C., Faust, D., Linstädter, J., 2008. Late Pleistocene and Holocene alluvial archives in the Southwestern Mediterranean: changes in fluvial dynamics and past human response. *Quat. Int.* 181, 39–54.